J Polym Res (2017) 24: 59
DOI 10.1007/s10965-017-1222-7

ORIGINAL PAPER

Facile fabrication approach for a novel multifunctional superamphiphobic coating based on chemically grafted montmorillonite/Al_2O_3-polydimethylsiloxane binary nanocomposite

Ruixia Yuan[1] · Shiqi Wu[1] · Huaiyuan Wang[1] · Lin Hu[1] · Yanji Zhu[1] · Simeng Gao[1] · Yixing Zhu[1] · Xiguang Zhang[1]

Received: 27 December 2016 / Accepted: 15 March 2017 / Published online: 23 March 2017

Abstract In this paper, a novel multifunctional superamphiphobic coating for anticorrosion was successfully prepared on aluminum substrate via a simple spraying technique. Al_2O_3 nanoparticles were chemically grafted onto montmorillonite (MMT) nanosheets via coupling effect of NH_2-C_3H_6-$Si(OC_2H_5)_3$ (KH-550) and then modified by low surface energy material polydimethylsiloxane (PDMS). The ethylene tetrafluoroethylene (ETFE) composite coating with 25 wt% MMT/Al_2O_3-PDMS binary nanocomposite exhibited well-designed nano/μ structures and possessed superamphiphobicity with high contact angles towards water (164°), glycerol (158°) and ethylene glycol (155°). This coating demonstrated outstanding self-cleaning ability and strong adhesive ability (Grade 1 according to the GB/T 9286). The superhydrophobicity could be maintained after 8000 times abrasion or annealing treatment for 2 h under 350 °C. The coating still retained high water-repellence after immersion in 1 mol/L HCl (146°), 1 mol/L NaOH (144°) and 3.5 wt% NaCl (151°) solutions for 30 d. It should be noted that this superamphiphobic coating revealed excellent long-term corrosion protection with extremely low corrosion rate (4.3×10^{-3} μm/year) and high protection performance (99.999%) after 30 d immersion in 3.5 wt% NaCl solutions based on electrochemical corrosion measurements. It is believed that such integrated functional coating could pave new way for self-cleaning and anticorrosion applications under corrosive/abrasive environment.

Keywords Superamphiphobic coating · Montmorillonite/Al_2O_3-polydimethylsiloxane nanocomposite · Self-cleaning · Wear/heat-resistance · Corrosion protection

Introduction

The ubiquitous corrosion and rusting could cause enormous resources wastes and economic loss to modern industrial societies [1]. Various anticorrosive paints have been developed to regulate metal corrosion, such as epoxy [2], polyester [3] and polyurethane [4], etc. Nevertheless, these traditional coatings are (super) hydrophilic, which are not durable owing to the easily permeation of corrosive ions (such as Cl^-) to the coating/metal interface. In recent years, superamphiphobic (super-repellent) coatings with high contact angle (CA > 150°) towards water and various oil liquids, inspired by the natural self-cleaning lotus leaf, have been studied for various applications, such as self-cleaning, anticorrosion and anti-icing [5–7]. Up to now, different technologies have been developed for fabricating superamphiphobic surfaces including chemical vapor deposition, electrodeposition, sol-gel processing and spraying [8–11]. However, most of these methods usually request complicated conditions, special devices and small substrate size, limiting their widespread industrial applications. Meanwhile, a common weakness of the current coatings is the susceptibility to mechanical abrasion or highly corrosive environment which could lead to the loss of non-wetting property [12, 13]. Hence, the scale-up practical applications of

Electronic supplementary material The online version of this article (doi:10.1007/s10965-017-1222-7) contains supplementary material, which is available to authorized users.

✉ Ruixia Yuan
yuanruixia663@126.com

✉ Huaiyuan Wang
wanghyjiji@163.com

[1] Provincial Key Laboratory of Oil & Gas Chemical Technology, College of Chemistry and Chemical Engineering, Northeast Petroleum University, Daqing 163318, China

superamphiphobic coatings are extremely scarce in aggressive service environment.

It is well-recognized that creating superamphiphobic surfaces is governed by both suitable hierarchical surface structures and extremely low surface free energy [14, 15]. Polydimethylsiloxane (PDMS) with low surface energy (21.6 mN/m) has been used to fabricate (super)hydrophobic surfaces mainly as biomimicking template or (super)hydrophobic modifier of nano/μ coating fillers, such as SiO_2, $CaCO_3$ and ZnO [16, 17]. Kapridaki et al. [18] incorporated PDMS with mixture of tetraethoxysilane and titanium-tetra-isopropoxide to form a uniform sol via sol-gel process, and brushed the solution on marble surfaces to obtain hydrophobic TiO_2-SiO_2-PDMS nanocomposite coating. Chakradhar et al. [19] prepared superhydrophobic coating with water contact angle (WCA) of 155° based on PDMS-modified ZnO nanocomposite by spraying technique. Gao et al. [20] added SiO_2 particles into PDMS solution to develop PDMS-SiO_2 uniform nano-suspensions, and then immersed clean glass slides into the solution to achieve superhydrophobic surfaces. However, these surfaces still cannot reach superamphiphobicity, and the coating robustness which is significant for industrial application is rarely investigated. Therefore, engineering superamphiphobic coatings with mechanically and chemically durability to apply as robust and anticorrosion barrier is especially required for practical applications.

Combination of nanoparticles with 2D nanosheets which have large surface area is theoretically possible to obtain essential roughness and also improve the barrier effect to prevent aggressive molecules from reaching the underneath substrate. Nine et al. [21] formulated a mixture suspension of reduced graphene oxide (rGO), diatomaceous earth particles and TiO_2 nanoparticles and then modified with PDMS, achieving highly superhydrophobic surface (WCA = 170 ± 2°) due to the structural improvement with hierarchical surface roughness. However, its application is limited by the complicated preparation technology and high cost of rGO [22]. Low-cost montmorillonite (MMT) nanosheets have been demonstrated to increase the length of the diffusion pathways for water, oxygen and aggressive ions and thus enhance the coating anticorrosion ability [23]. Lai et al. [24] fabricated MMT/polyacrylate coating which showed better corrosion protection efficiency over neat polyacrylate on the basis of electrochemical measurements. Zhang et al. [25] found that the polyaniline/MMT/epoxy composite coating exhibited superior barrier ability compared with PANI/epoxy coating. Unfortunately, MMT with merely 2D sheet nanostructure is difficult to build structural hierarchy for superamphiphobic coating. To achieve extremely high roughness, nanoparticles could be grafted via chemical bonding function onto the MMT nanosheets surface, but not directly mixed with MMT. Meera et al. [26] prepared SiO_2/MMT composites via in situ polymerization of tetraethylorthosilicate precursor in the presence of MMT. However, the involved complicated steps and particularly long polymerization time made challenges for large-scale applications.

In this study, we aim to develop a facile technique to prepare binary system of MMT nanosheets/Al_2O_3 nanoparticles composite by the coupling effect of NH_2-C_3H_6-Si(OC_2H_5)$_3$ (KH-550) and low-surface-energy modification of PDMS. KH-550 could react with both the hydroxyl groups of MMT and Al_2O_3 surface, leading to the graft of Al_2O_3 nanoparticles onto MMT nanosheets surface. Furthermore, the use of traditional hydrophilic film-forming materials, such as epoxy, polyurethane, acrylic resins, may cause the loss of coating non-wetting property after abrasion/corrosion mainly because of hydrophilic impurities left on the surface [27, 28]. Thus, in this work the inert hydrophobic fluorinated polymer ethylene tetrafluoroethylene (ETFE) is introduced as film-forming material of the prepared robust superamphiphobic coating due to its advantages of low surface energy, high thermal stability, self-lubrication, excellent mechanical strength and chemical resistance to acids, bases and solvents [29, 30]. The as-prepared MMT/Al_2O_3-PDMS nanocomposite was embedded into the ETFE coating as nanofiller to build the requisite hierarchy bionic structures. 1*H*,1*H*,2*H*,2*H*–perfluorooctyltriethoxysilane (POTS) which has extremely low surface energy (19 mN/m) was also added into the composite coating to achieve superamphiphobic surface. To enhance the adhesion strength between coating and metal surface, nano/μ structures were built on the aluminum surface by acid etching and hydrothermal reaction. The superamphiphobic coating with excellent mechanical durability and corrosion resistance was finally successfully prepared on the etched aluminum substrate via simple spraying approach which could be widely applied in industry. The durable non-wettability, self-cleaning, wear resistance and thermal stability of the composite coating were investigated in detail. The anticorrosion behaviors were analyzed based on electrochemical corrosion measurement in saline conditions. It is believed that this work will provide a new way for multifunctional anticorrosion coating which could be potentially widely used in practical application.

Material and methods

Materials

Commercial ETFE powders were provided by DuPont (USA). MMT nanosheets with diameter ranging from 500 nm to 2 μm were purchased from Shenzhen Haicheng Co. Ltd. (China). Ethylene glycol, glycerol, ethyl acetate, ethanol and Al_2O_3 nanoparticles with average diameter of about 30 nm were supplied from Aladdin Reagent Co. Ltd. (China). POTS was purchased from Sigma Aldrich Co. (USA). Hydroxyl-terminated PDMS (purity ≥98 wt%) and KH-550 were obtained from Jinan Hailan Reagent Factory and Jinan Xingfeilong Chemical Ltd. (China), respectively. The

composition of aluminum plate used in this work is 99.0% Al, 0.45% Si, 0.05–0.20% Cu, 0.01% Zn, 0.035% Mn,0.05% V and 0.35% Fe.

Preparation of MMT/Al_2O_3-PDMS composite

The MMT/Al_2O_3-PDMS composite was prepared as follows: 1 g MMT nanosheets and 1 g Al_2O_3 nanoparticles were added into a 50 mL mixture solution of deionized water, KH-550 and ethanol (*v*/v/v = 1/1/18) under ultrasonication for 30 min, followed by dissolving 0.5 mL PDMS with magnetic stirring for 24 h at room temperature. After filtration and drying, the superhydrophobic MMT/Al_2O_3-PDMS composite was finally obtained. As illustrated in Fig. 1a, through siloxane bonding the hydroxyl groups of MMT and Al_2O_3 surface firstly reacted with KH-550 and then the Al_2O_3 nanoparticles could graft on the MMT nanosheets surface. The hydroxyl-terminated PDMS could finally bond with the MMT/Al_2O_3 composite to lower the surface free energy.

Preparation of ETFE-MMT/Al_2O_3-PDMS composite coating

The pristine aluminum plate (1100 grade, 80 mm × 80 mm × 1 mm) was polished with 1000 mesh sand papers in one direction, and then ultrasonically washed in absolute alcohol. Afterwards, the plate was etched in hydrochloric acid (3 mol/L) for 30 min followed by absolutely washing with deionized water to remove oxidation residue. The pre-treated aluminum with nano/μ roughness was eventually achieved by a boiling water bath for 30 min (Fig. 1b).

1 g ETFE powders, certain amount of MMT/Al_2O_3-PDMS and 0.2 g POTS were added into 20 mL ethyl acetate and unltrasonicated for 60 min to ensure a uniform dispersion. The superamphiphobic coating was obtained by spraying the above solution on the pre-treated aluminum plate with an air spray gun under a pressure of 0.3 bar and curing under 330 °C for 1.5 h (Fig. 1b). The composite coating with unmodified MMT and Al_2O_3 nanoparticles was also prepared via the same procedures as control samples.

Characterization

The wettabilities of the composite coatings were evaluated by measuring the CAs and sliding angles (SAs) with approximately 5 μL liquid droplets using Contact Angle Meter (JGW-360A, Chengdeshi Shipeng Detection Equipment Co. Ltd., China). The coating morphologies were observed using a Zeiss SIGMA field emission scanning electron microscope (SEM). The coating surface roughness was examined using the laser scanning confocal microscope (LSCM) (LEXTOLS3000, OLYPUS, Japan). The chemical composition was inspected by Tensor27 fourier transform infrared spectroscopy (FT-IR) and X-ray energy dispersive spectrometry (EDS) using an Oxford Instruments. The adhesive

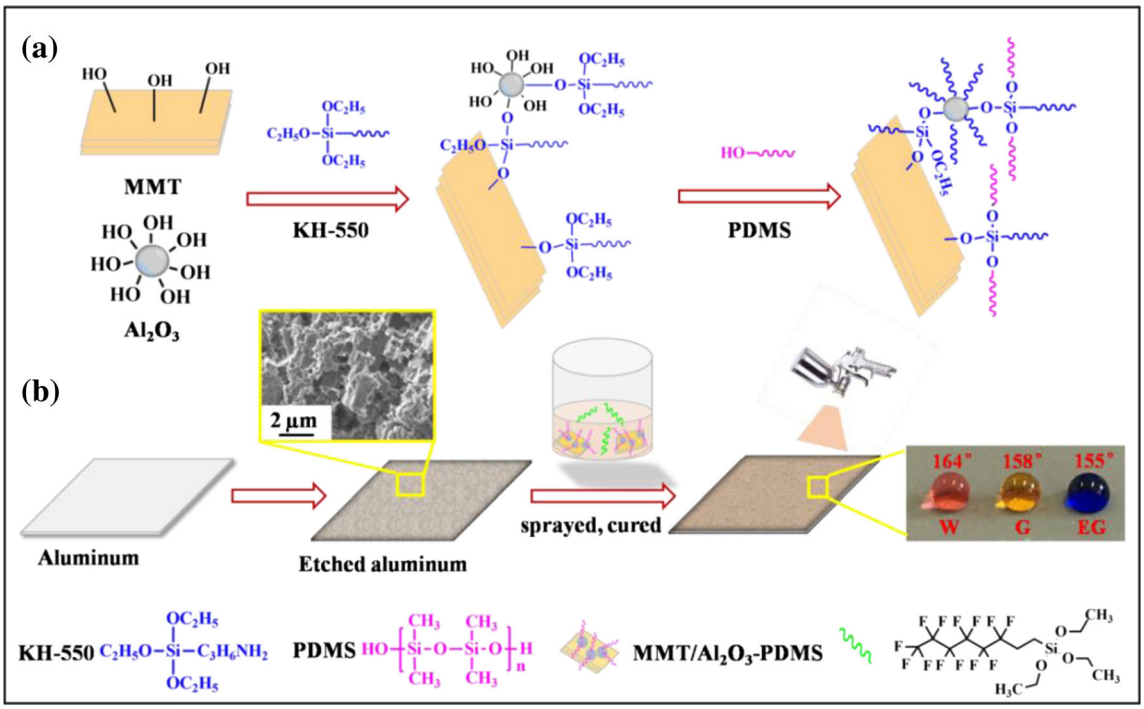

Fig. 1 Schematic illustration of the preparation procedures for MMT/Al_2O_3-PDMS nanocomposite (**a**) and the superamphiphobic ETFE-MMT/Al_2O_3-PDMS composite coating (**b**). The pink, yellow and blue droplets on the coating surface represent water (W), glycerol (G) and ethylene glycol (EG) droplets, respectively

strength of the composite coating was investigated using cross-cut method based on GB/T 9286 standard testing method. The wear-resistant ability of the coating was evaluated using Taber Wear and Abrasion Testers (JST-3393). Thermogravimetric (TG) data were obtained by thermogravimetric analyzers (STA73000, Beijing SaiSiMeng Instruments Co., Ltd., China) at a heating rate of 10 °C/min under air atmosphere. The variation of WCAs was investigated after immersing the coatings into strongly acidic (1 mol/L HCl), alkaline (1 mol/L NaOH) and 3.5 wt% NaCl aqueous solutions for 30 d. To prevent the corrosive medium from penetrating the coatings through the defect region on the edge, the uncoated side and the edge of the samples were sealed using paraffin before anticorrosion tests. The electrochemical corrosion measurement was conducted in 3.5 wt% NaCl solution by employing electrochemical workstation (Autolab PGSTAT302N), with Pt sheet and saturated calomel electrode (SCE) as counter electrode and reference electrode respectively.

Results and discussion

Coating wettability

The modified and unmodified MMT/Al_2O_3 nanocomposite varying from 0 to 30 wt% was added into the ETFE coatings to optimize the coating non-wettabilities. The average thicknesses of the prepared coatings range from 30 to 50 μm (Table S1, S2). The variations of CAs and SAs to various liquids (water, glycerol and ethylene glycol) for ETFE-MMT/Al_2O_3-PDMS composite coatings on the etched aluminum substrates were shown in Fig. 2a,b. The non-wetting ability of the composite coating can be enhanced significantly with the addition of MMT/Al_2O_3-PDMS nanocomposite, as evidenced by the increasing CAs and decreasing SAs to water, glycerol and ethylene glycol. The best superamphiphobic property can be achieved by the coating with 25 wt% MMT/Al_2O_3-PDMS, which has average CAs of 164°, 158°, 155° and SAs of 0.7°, 3.2°, 3.9° towards water, glycerol and ethylene glycol, respectively. It should be pointed out that the superamphiphobicity could not be achieved for the ETFE-MMT/Al_2O_3-PDMS composite coated on unetched smooth aluminum substrates (Fig. S1), indicating the necessity of rough surface structure of aluminum substrates for the superamphiphobicity of the composite coating. Even though the addition of unmodified MMT/Al_2O_3 could also improve the anti-wettability of the composite coatings towards water, glycerol and ethylene glycol, the best result obtained from the composite coating with 25 wt% unmodified MMT/Al_2O_3 showed superior repelling properties toward water (153°) and glycerol (151°) but failed to ethylene glycol (139°) (Fig. 2c). The composite coatings with 25 wt% modified MMT/Al_2O_3-PDMS and unmodified MMT/Al_2O_3 were named as ETFE-MMT/Al_2O_3-PDMS-25 and ETFE-MMT/Al_2O_3–25 respectively and were further investigated in detail in the following studies. It should be noted that the ETFE-MMT/Al_2O_3-PDMS-25 composite coating demonstrated better water-repellent ability with high CAs (158–164°) than the ETFE-MMT/Al_2O_3–25 composite coating with CAs (150–154°) towards corrosive solutions from pH 1 to 14 (Fig. 2d).

Fig. 3a showed different sized water drops on the ETFE-MMT/Al_2O_3-PDMS-25 composite coating and all the water drops exhibited a near-perfect spherical shape. The coating non-wettability towards flowing fluid is essential for practical application. As shown in Fig. 3b, the water jet reflected from the impact point at 45°, without spreading on the surface. The water jet was directed onto the overall coating surface for at least 30 min, and the WCA still remained 162°, indicating the stability of the ETFE-MMT/Al_2O_3-PDMS-25 composite coating. To study the self-cleaning property of the composite coating, an abundant amount of graphite powder was spread on coating surface and water was slowly dripped onto the polluted surface (Fig. 3c). It can be displayed that the initial water drops picked up nearly all the graphite powder they encountered, and were coated by a heavy layer of dirt. These drops rolled off the coating surface and simultaneously removed the graphite dirt. The followed water drops cleaned the coating surface completely, showing excellent self-cleaning ability of the superamphiphobic coating. Such excellent stability and self-cleaning ability could provide possibility for long-term practical applications in rigorous environment.

Coating morphologies

As displayed in Fig. 4a, the original MMT nanosheet was very smooth before modification. Without the silane coupling agent KH-550, the MMT/Al_2O_3 powders are superhydrophilic and Al_2O_3 particles could not graft onto the MMT surface (Fig. S2). While through siloxane bonding effect assisted by KH-550, the hydroxyl-terminated Al_2O_3 nanoparticles can successfully graft on the MMT surface as observed in Fig. 4b. After modification, nearly spherical water droplets could stand on the surface of MMT/Al_2O_3-PDMS composite, indicating the transformation from superhydrophilic property (WCA = 10 ± 2°) to super-repellence towards water (WCA = 156 ± 1.5°) due to the low-surface-energy modification by PDMS (Inset of Fig. 4a,b). Compared with merely physical mixing of MMT and Al_2O_3 in the composite coating, the incorporation of chemically modified MMT/Al_2O_3-PDMS could result in highly porous and rough surface (Fig. 4c,d). The LSCM result showed that the average surface roughness value (Ra) of ETFE-MMT/Al_2O_3-PDMS-25 coating was 1.74 μm, which is higher than that of ETFE-MMT/Al_2O_3–25 coating (1.51 μm) (Fig. 4e,f). The improved roughness could lead to the superior water repellence for ETFE-MMT/Al_2O_3-PDMS-25 coating with higher WCA of 164° than that of ETFE-MMT/Al_2O_3–25 coating (154°). It should be pointed out that the ETFE-MMT/Al_2O_3-PDMS-25

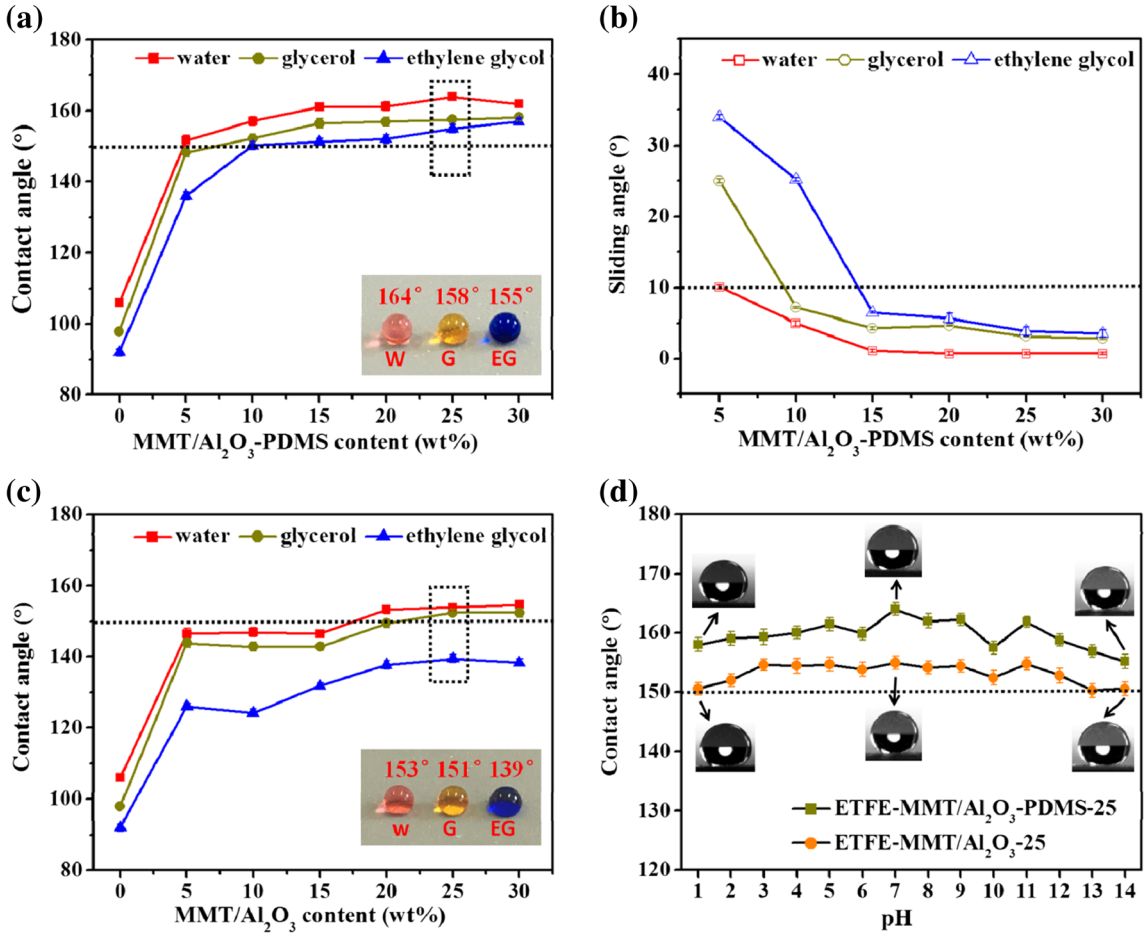

Fig. 2 Effect of MMT/Al_2O_3-PDMS content on the contact angles (**a**) and sliding angles (**b**) of the ETFE-MMT/Al_2O_3-PDMS composite coatings. Effect of MMT/Al_2O_3 content on the contact angles of the ETFE-MMT/Al_2O_3 composite coatings (**c**). Effect of solution pH on the water contact angles of the composite coatings (**d**). Inset: optical image of water (W), glycerol (G) and ethylene glycol (EG) droplets on the coating surface

composite coating could achieve superamphiphobicity, while the ETFE-MMT/Al_2O_3–25 cannot reach super-repellence to ethylene glycol as reflected in Fig. 2. This could be mainly attributed to both the higher rough structures and lower free surface energy by introducing superhydrophobic MMT/Al_2O_3-PDMS composite.

Chemical analysis

As shown in Fig. 5a, pure Al_2O_3, MMT and modified MMT/Al_2O_3-PDMS composite were further characterized by FT-IR. For the spectrum of MMT/Al_2O_3-PDMS, the absorption bands at 1611, 790 and 580 cm^{-1} were associated with the -OH stretching vibration, the Al-O stretching vibration and the stretching mode of six-coordinated Al originated from MMT and Al_2O_3, respectively [31, 32]. The strong adsorption peak located at 1099 cm^{-1} corresponded to the stretching vibration of Si-O in MMT and PDMS molecules [25]. The new absorption band observed at 1264 cm^{-1}, related to the stretching vibration of the -CH_3 groups in -Si-(CH_3), were generated from the modification by PDMS [18]. As evidenced by the EDS result of MMT/Al_2O_3-PDMS (Fig. 5c), the composite was mainly composed of Al, O, Si and C. The appearance of Si should be attributed to MMT and the successful modification of PDMS.

As for the spectrum of ETFE-MMT/Al_2O_3-PDMS-25 composite coating (Fig. 5b), the strong adsorption bands at 1240 and 1149 cm^{-1} were associated with the stretching vibration of -CF_2, which were originated from ETFE and POTS molecules. The peak at 2933 cm^{-1} should be related to asymmetric C-H stretching of POTS or ETFE. The bands located at 1611 (−OH stretching vibration) and 642 cm^{-1} (−CH_2 in plane vibration) were mainly generated from MMT/Al_2O_3-PDMS composite and ETFE molecules, respectively [30]. Fig. 5d displayed the EDS spectra of the ETFE-MMT/Al_2O_3–25 and ETFE-MMT/Al_2O_3-PDMS-25 composite coatings. The fluorine content (28.4%) of ETFE-MMT/Al_2O_3-PDMS-25 is relatively lower than that of ETFE-MMT/Al_2O_3–25 composite coating

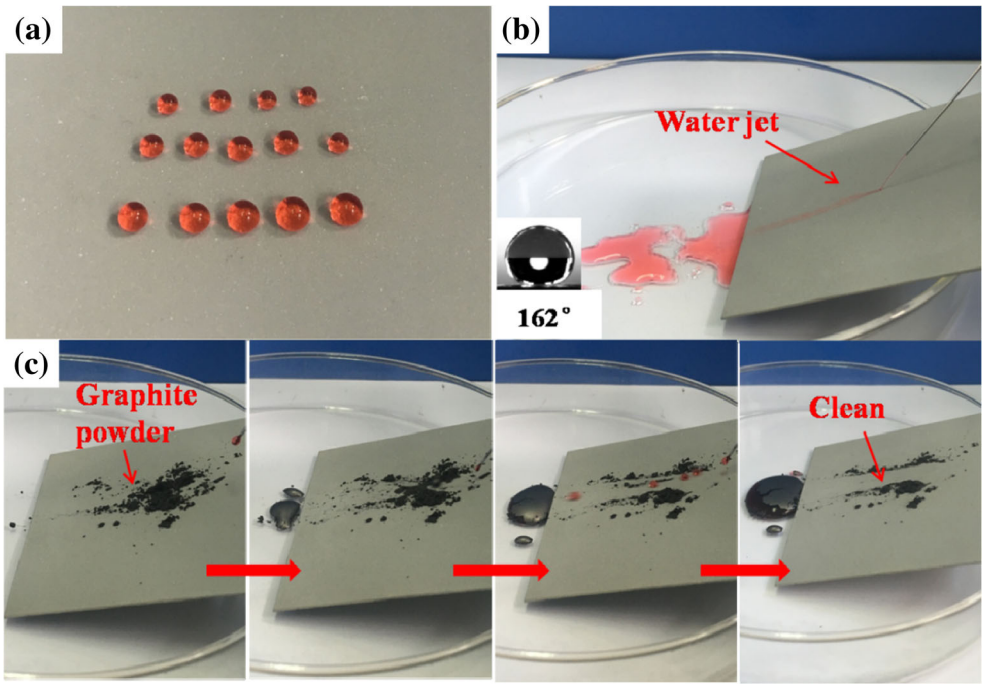

Fig. 3 Optical image of water drops on the ETFE-MMT/Al_2O_3-PDMS-25 composite coating (**a**), water jet impact (**b**) and the self-cleaning performance of the coating (**c**)

(49.7%), even though the former coating possessed superior non-wettability. This indicated that both low free surface energy and high roughness are essential for building superamphiphobic surface.

Mechanical behaviors of the prepared coating

Adhesion ability

The adhesive strength of the ETFE-MMT/Al_2O_3–25 and ETFE-MMT/Al_2O_3-PDMS-25 composite coatings was investigated (Fig. 6). The composite coatings were first scribbled into 2 mm × 2 mm girding by using a razor to expose the coating substrate, and then the test tapes were pressed and pulled from the tested surface within 5 min. As shown in Fig. 6a1,a2, there were some detachment of flakes on the ETFE-MMT/Al_2O_3–25 composite coating and the impacted area was between 5% and 15%, which can be classified as Grade 2. However, the adhesion strength of the ETFE-MMT/Al_2O_3-PDMS-25 composite coating was improved to Grade 1, which showed excellent adhesion with little peeling in the cross-incision (Fig. 6 b1,b2). The strong interface adhesive strength could be attributed to nano/μ-scaled roughness of the etched aluminum substrate as well as chemically bonded MMT/Al_2O_3-PDMS nanofillers. Furthermore, it should be pointed out that the coating with modified MMT/Al_2O_3-PDMS composite could still remain superamphiphobicity after the cross-cut test as shown in Fig. 6 b3, while the ETFE-MMT/Al_2O_3–25 coating lost its super-repellence towards water, ethanol and ethylene glycol in the cross cut area (Fig. 6 a3).

Wear resistance

To estimate the wear-resistance of the composite coatings, the abrasion resistance test was performed. As displayed in Fig. 7a, the friction wheels were covered by 1000 mesh sand paper and the composite coating was fixed under the friction wheels with 100 kPa. The ETFE-MMT/Al_2O_3-PDMS-25 coating could still remain superhydrophobicity with WCA of 151° after 8000 times rubbing, while the ETFE-MMT/Al_2O_3–25 composite coating lost its superhydrophobicity with WCA of 142°. Furthermore, the ETFE-MMT/Al_2O_3–25 composite coating showed serious damage after 19,000 cycles and the WCAs decreased from 154° to 130° (Fig. 7b). Comparatively, the ETFE-MMT/Al_2O_3-PDMS-25 composite coating exhibited slight damage even after 35,000 times abrasion with WCA of 142° left. The enhanced abrasive resistance of ETFE-MMT/Al_2O_3-PDMS-25 composite coating can be attributed to the addition of modified MMT/Al_2O_3-PDMS which could design better internal and external nano/μ structures. Moreover, ETFE macromolecules with high ductility (400%) and self-lubrication property were also benefit for the superamphiphobic coating to undergo long-time abrasion [30]. Such robust surface would have wide application prospects in rigorous practical application.

Heat resistance

The thermal stability of the ETFE-MMT/Al_2O_3-PDMS-25 and ETFE-MMT/Al_2O_3–25 composite coatings was examined by TG analysis. As shown in Fig. 8a, both the coatings presented a stable thermal state under 400 °C and the weight

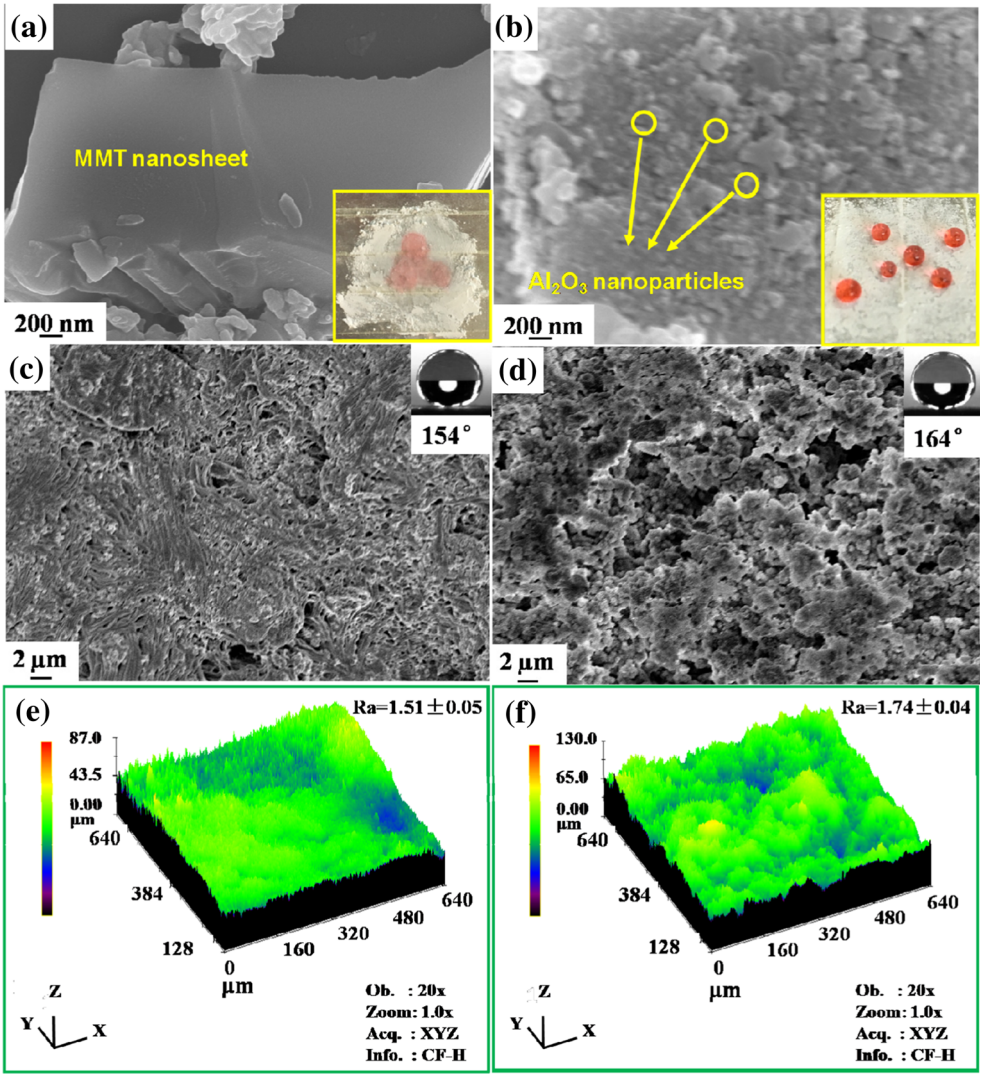

Fig. 4 SEM images of MMT nanosheet (**a**), MMT/Al_2O_3-PDMS nanocomposite (**b**), ETFE-MMT/Al_2O_3–25 (c) and ETFE-MMT/Al_2O_3-PDMS-25 (d) composite coatings. LSCM images of ETFE-MMT/Al_2O_3–25 (**e**) and ETFE-MMT/Al_2O_3-PDMS-25 (**f**) composite coatings. Inset: the water drops on the surface of unmodified MMT (**a**), MMT/Al_2O_3-PDMS (**b**), the ETFE-MMT/Al_2O_3–25 (**c**) and ETFE-MMT/Al_2O_3-PDMS-25 (**d**) composite coatings

loss was less than 2.6%. Such excellent heat-resistance can be attributed to the high bonding energy of CF_2 bonds in ETFE macromolecules. After annealing treatment for 2 h, both the coatings could maintain superhydrophobicity under 350 °C, while lose their anti-wetting ability at above 400 °C (Fig. 8b). Comparably, the ETFE-MMT/Al_2O_3-PDMS-25 composite coating possessed higher water repellence than the ETFE-MMT/Al_2O_3–25 composite coating. The stable anti-wettability over a wide temperature range could provide application possibility in special high temperature environment.

Anticorrosion performance of the prepared coating

Corrosion resistance against corrosive solutions

To study the barrier effect of the coatings, the aluminum specimens with ETFE-MMT/Al_2O_3–25 and ETFE-MMT/Al_2O_3-PDMS-25 composite coatings were subjected to long-term immersion in highly corrosive solutions. As shown in Fig. 9a, the ETFE-MMT/Al_2O_3-PDMS-25 composite coating retained high super(hydrophobicity) with WCAs of 146°, 144° and 151° after immersion in 1 mol/L HCl, 1 mol/L NaOH and 3.5 wt% NaCl solution for 30 d, respectively. Meanwhile, apparent silver mirror effect can be observed on the coating surface owing to its high water repellent ability. However, the ETFE-MMT/Al_2O_3–25 composite coating was seriously damaged even after only 10 d immersion in 1 mol/L HCl, 1 mol/L NaOH and 3.5% NaCl solution, left extremely low WCAs of 6°, 15° and 106°, respectively (Fig. 9b). The SEM images after anticorrosion tests (Fig. S3) showed that nano/μ structures can be maintained for the ETFE-MMT/Al_2O_3-PDMS-25 coating, while significant corrosion or crack can be found for the ETFE-MMT/Al_2O_3–25 coating. The superior and durable anticorrosion ability of ETFE-MMT/Al_2O_3-PDMS-25 coating compared to ETFE-MMT/Al_2O_3–25 coating can be mainly due to the addition of chemically modified MMT/Al_2O_3-PDMS nanocomposite which could build stable and highly porous nano/μ structures as better barrier surface to prevent the corrosive ions from permeation.

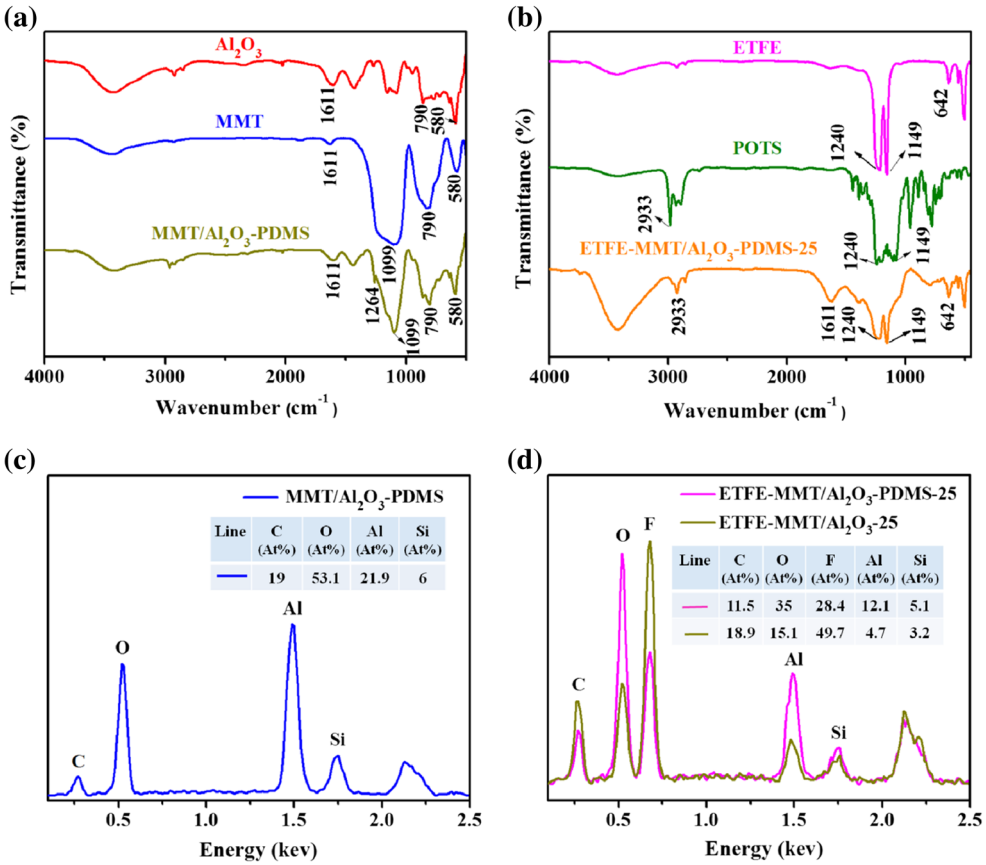

Fig. 5 FT-IR spectra of pure Al_2O_3, MMT and MMT/Al_2O_3-PDMS nanocomposite (**a**), POTS, ETFE and ETFE-MMT/Al_2O_3-PDMS-25 composite coating (**b**) and EDS spectra of MMT/Al_2O_3-PDMS nanocomposite (**c**), ETFE-MMT/Al_2O_3–25 and ETFE-MMT/Al_2O_3-PDMS-25 composite coatings (**d**)

Potentiodynamic polarization analysis

In order to investigate the corrosion protection efficiency of the coatings, Tafel plots for pure Al and coated Al substrates were characterized in 3.5 wt% NaCl aqueous solutions (Fig. 10). Furthermore, the electrochemical parameters acquired from the polarization curves (Table 1) could also provide an indication of the coating stability during exposure to salty corrosive environment. Typically, positive shift of corrosion potential (E_{corr}) represents lower thermodynamical corrosion tendency and smaller corrosion current (I_{corr}) value means lower corrosion dynamic rate [33, 34]. Compared with the I_{corr} of untreated Al substrate (8.7×10^{-5} A/cm^2), the ETFE-MMT/Al_2O_3–25 composite coating revealed reduced corrosion rate with lower I_{corr} of 1.1×10^{-7} A/cm^2 after 10 d immersion. The slight negative shift of E_{corr} indicated the

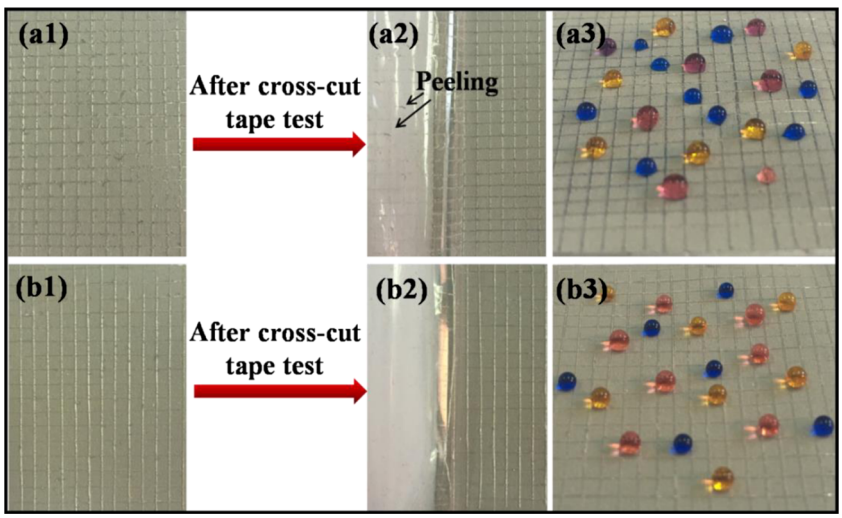

Fig. 6 Optical images of the ETFE-MMT/Al_2O_3–25 and ETFE-MMT/Al_2O_3-PDMS-25 composite coating before (**a1, b1**), after (**a2, b2**) cross-cut tape test and the water (*pink*), glycerol (*yellow*) and ethylene glycol (blue) droplets on the tested surfaces (**a3, b3**)

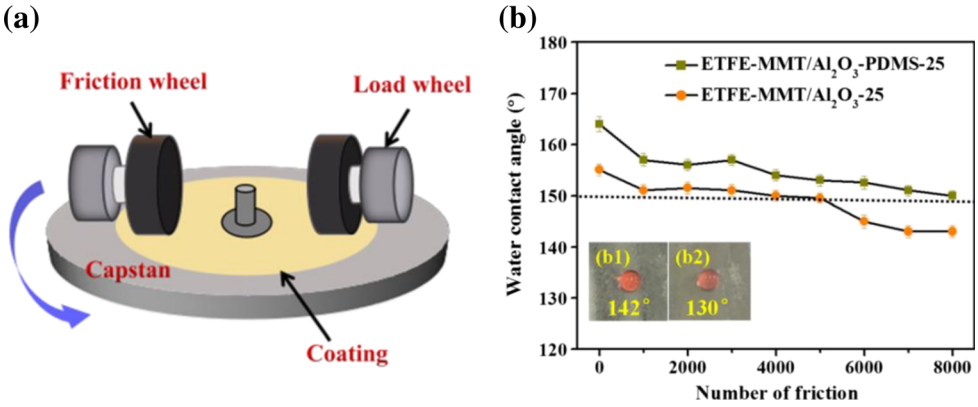

Fig. 7 Schematic illustration of the abrasion resistance test (**a**), influence of friction process on the water contact angles of the ETFE-MMT/Al_2O_3–25 and ETFE-MMT/Al_2O_3-PDMS-25 composite coatings (**b**). Inset: the optical images of water droplets on the ETFE-MMT/Al_2O_3-PDMS-25 coating after 35,000 cycles abrasion (b1) and ETFE-MMT/Al_2O_3–25 coating after 19,000 cycles abrasion (b2)

initiation of pitting corrosion, which could also be reflected by the loss of coating superhydrophobicity after 10 d immersion in 3.5 wt% NaCl solution. As for the ETFE-MMT/Al_2O_3-PDMS-25 coating, positive shift of E_{corr} (−706 mV) and extremely low corrosion current density (4.1×10^{-10} A/cm^2) were obtained after 30 d immersion in 3.5 wt% NaCl solution. This revealed the long-term anticorrosion performance of the coating, which can be mainly due to its durable and superior water-repellent ability as displayed in Fig. 9a.

The corrosion rate (CR) and corrosion protection efficiency (P.E.%) were obtained from the measured I_{corr} values according to Eqs. (1, 2) [5]:

$$CR = 3270 \times \frac{I_{corr} \cdot M}{V \cdot d} \quad (1)$$

$$P.E.\% = \left(1 - \frac{I^{c}_{corr}}{I^{0}_{corr}}\right) \times 100 \quad (2)$$

where 3270 = 0.01 × [1 year (in s)/96,497.8] and 96,497.8 = 1 F in Coulombs. M, V and d represent the atomic mass, the valence and the density of aluminum substrate, respectively. I^{0}_{corr} and I^{c}_{corr} were the corrosion current of bare Al substrate and coated Al substrate, respectively.

The ETFE-MMT/Al_2O_3-PDMS-25 composite coating exhibited durable corrosion resistance property with extremely lower corrosion rate (4.3×10^{-3} μm/year) and higher protection performance (99.999%) after 30 d immersion compared to the ETFE-MMT/Al_2O_3–25 coating with corrosion rate (1.3 μm/year) and protection performance (99.874%) after 10 d immersion. The enhanced corrosion protection performance of the ETFE-MMT/Al_2O_3-PDMS-25 coating should be related the addition of modified MMT/Al_2O_3-PDMS nanocomposite which provided better barrier effect.

Electrochemical impedance spectroscopy (EIS) analysis

The EIS spectra for the composite coatings after immersion in 3.5 wt% NaCl solution were investigated to quantify their corrosion resistant performance and unveil the anticorrosion mechanism. Lower semicircle diameter in Nyquist spectra (charge transfer resistance) corresponds to higher corrosion rate [34]. As displayed in Fig. 11a,b, the ETFE-MMT/Al_2O_3–25 composite coating possessed much lower total impedance magnitude after 10 d immersion than that of ETFE-MMT/Al_2O_3-PDMS-25 composite coating after 30 d immersion, which could be attributed to the penetration of corrosive chloride ions to the coating/aluminum interface and initiation of localized corrosion as reflected in Tafel plot (Fig. 10). The impedance spectra of ETFE-MMT/Al_2O_3-PDMS-25 coating exhibited basically one semicircle over the whole frequency range after 30 d immersion which implied a capacitive behavior and barrier type protection.

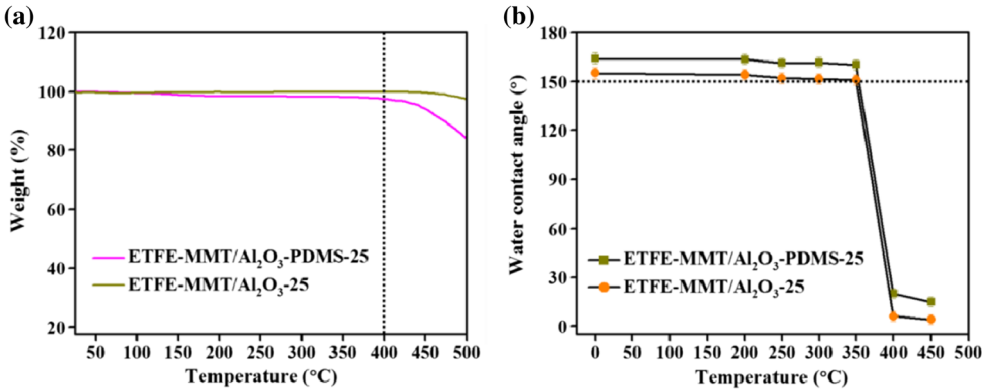

Fig. 8 TG spectra (**a**) and wettability (**b**) of the ETFE-MMT/Al_2O_3–25 and ETFE-MMT/Al_2O_3-PDMS-25 composite coatings

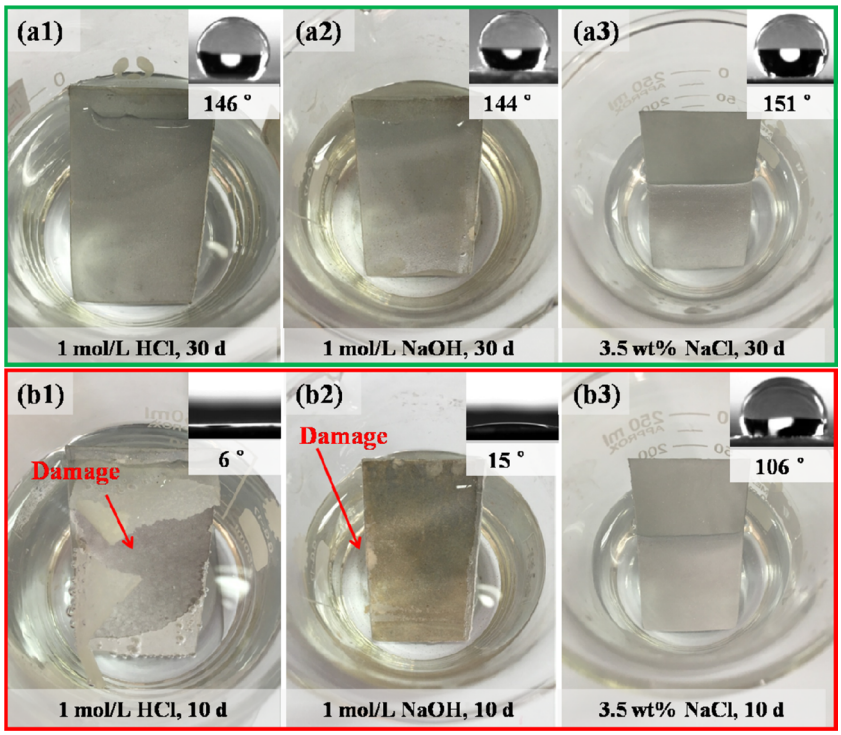

Fig. 9 Optical images of the ETFE-MMT/Al_2O_3-PDMS-25 (**a1, a2, a3**) and ETFE-MMT/Al_2O_3–25 (**b1, b2, b3**) composite coatings after immersion in different corrosive solutions

In Bode plots, the impedance modulus at the lowest measured frequency (most commonly $|Z|_{0.01\ Hz}$) has been frequently tracked as a semi-quantitative indicator of coating's barrier function [35]. In Fig. 11c,d, the $|Z|_{0.01\ Hz}$ value of ETFE-MMT/Al_2O_3-PDMS-25 coating (~10^7 Ω/cm^2) after 30 d immersion was about two orders higher than that of ETFE-MMT/Al_2O_3–25 coating (~10^5 Ω/cm^2) after 10 d immersion, indicating the better barrier property of the former coating. The long-term stable anticorrosion performance of the ETFE-MMT/Al_2O_3-PDMS-25 coating could be also reflected by the higher phase angles (~90°) over a wide range in frequency after 30 d immersion (Fig. 11f).

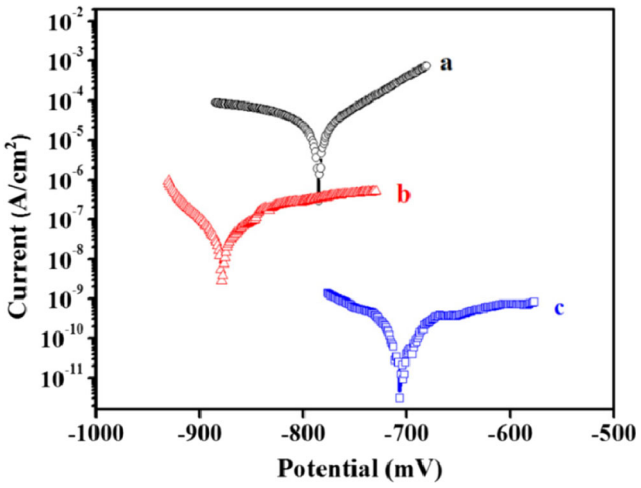

Fig. 10 Potentiodynamic polarization curves for the uncoated aluminum substrate (**a**), ETFE-MMT/Al_2O_3–25 coating after 10 d (**b**) immersion in 3.5 wt% NaCl solution and ETFE-MMT/Al_2O_3-PDMS-25 coating after 30 d (**c**) immersion in 3.5 wt% NaCl solution

Comparatively, for the phase diagrams of ETFE-MMT/Al_2O_3–25 coating, the existence of two time constants at high and low frequencies was evident and indicated that corrosion has already occurred on the electrolyte/substrate interface (Fig. 11e) [36].

It should be noted that the ETFE-MMT/Al_2O_3-PDMS-25 composite coating could maintain superhydrophobicity with WCA of 151° even after immersion in 3.5 wt% NaCl solution for 30 d (Fig. 9 a3). However, the ETFE-MMT/Al_2O_3–25 composite coating lost its super-repellence towards 3.5 wt% NaCl solution with WCA of only 106° after 10 d immersion (Fig. 9b3). The higher rough surface of ETFE-MMT/Al_2O_3-PDMS-25 composite coating with nano/μ structures could trap enough air at the solid-liquid interface and offer a stable air layer to prevent the penetration of corrosive chloride ions and water through the coating. Furthermore, compared to mere simple mix of unmodified Al_2O_3 and MMT in ETFE-MMT/Al_2O_3–25 coating, the modified MMT/Al_2O_3-PDMS binary system via chemical bonding used in ETFE-MMT/Al_2O_3-PDMS-25 composite coating could increase the length of the diffusion pathways for water and chloride ions and thus enhance the coating barrier effect [25]. In consequence, the ETFE-MMT/Al_2O_3-PDMS-25 composite coating with superior and durable anti-wettability could achieve much better anticorrosion ability.

Conclusions

In this work, we prepared superhydrophobic MMT/Al_2O_3-PDMS nanocomposite through the coupling effect of KH-

Table 1 Potentiodynamic polarization parameter values for uncoated and coated Al substrates

Sample	Immersion time	E_{corr} (mV)	I_{corr} (A/cm^2)	CR (μm/year)	P.E. (%)
Uncoated	0.5 h	−784	8.7×10^{-5}	1.0×10^{3}	—
ETFE-MMT/Al_2O_3–25	10 d	−879	1.1×10^{-7}	1.3	99.874
ETFE-MMT/Al_2O_3-PDMS-25	30 d	−706	4.1×10^{-10}	4.3×10^{-3}	99.999

550 and low-surface-energy modification of PDMS. With 25 wt% MMT/Al_2O_3-PDMS addition, superamphiphobic ETFE composite coating on etched aluminum substrate was successful achieved, with contact angles of 164°, 158° and 155° towards water, glycerol and ethylene glycol, respectively. The excellent self-cleaning ability to graphite powder could

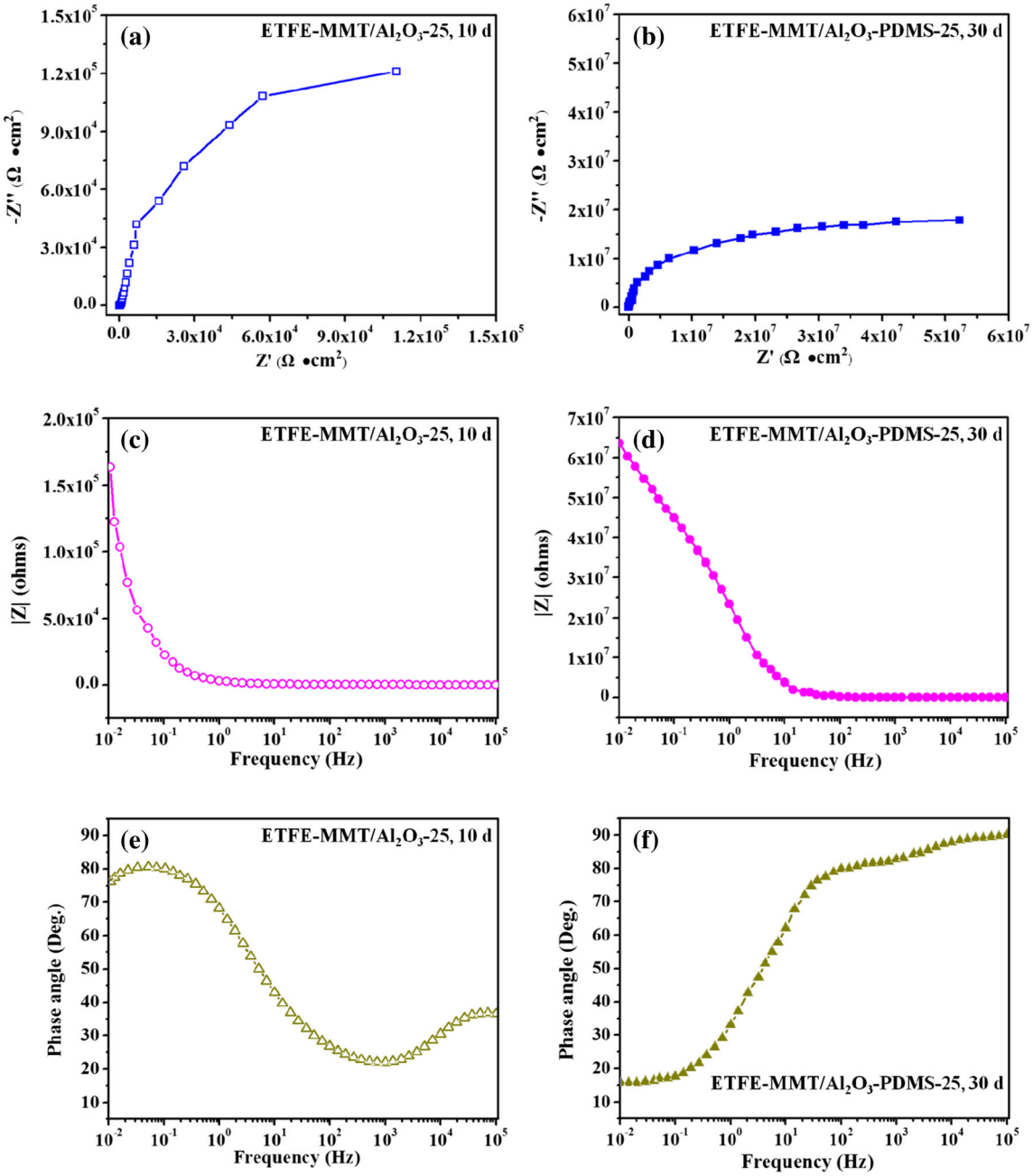

Fig. 11 Nyquist, Bode and phase plots of ETFE-MMT/Al_2O_3-PDMS-25 (**a, c, e**) and ETFE-MMT/Al_2O_3-PDMS-25 (**b, d, f**) composite coatings after immersion in 3.5 wt% NaCl solution for 10 d and 30 d, respectively

be attributed to the highly and stable water-repellence of the coating with well-designed nano/μ structures. The strong adhesion ability of the ETFE-MMT/Al_2O_3-PDMS-25 coating was also obtained due to the nano/μ-scaled roughness of the etched aluminum substrate and the chemical bonding effect between MMT nanosheets and Al_2O_3 nanoparticles. The ETFE-MMT/Al_2O_3-PDMS-25 coating demonstrated a remarkable improvement in wear resistance and higher WCAs in high temperature environment compared to the ETFE-MMT/Al_2O_3–25 coating. From the electrochemical measurements, the ETFE-MMT/Al_2O_3-PDMS-25 coating possessed extremely high protection performance (99.999%) and low corrosion rate (4.3×10^{-3} μm/year) even after 30 d immersion in 3.5 wt% NaCl solution. Based on the EIS analysis, the ETFE-MMT/Al_2O_3-PDMS-25 coating exhibited long-term anticorrosion performance mainly due to the chemical modified MMT/Al_2O_3-PDMS nanocomposite which could build durable superamphiphobic surface as better barrier and increase the length of diffusion pathways of water and chloride ions. It is believed that such robust multifunctional coating could have promising potential for long-term application in the corrosion protection of metal substrates.

Acknowledgements The research is financially supported by National Science Foundation of China (21507009, 21676052), Natural Science Foundation of Heilongjiang Province (B2016002, QC2015012) and Young Innovative Talent Training Program of Heilongjiang Province (UNPYSCT-2016083).

References

1. Peng C-W, Hsu C-H, Lin K-H, Li P-L, Hsieh M-F, Wei Y, Yeh J-M, Yu Y-H (2011) Electrochemical corrosion protection studies of aniline-capped aniline trimer-based electroactive polyurethane coatings. Electrochim Acta 58:614–620
2. Cubides Y, Castaneda H (2016) Corrosion protection mechanisms of carbon nanotube and zinc-rich epoxy primers on carbon steel in simulated concrete pore solutions in the presence of chloride ions. Corros Sci 109:45–161
3. Mirabedini SM, Kiamanesh A (2013) The effect of micro and nano-sized particles on mechanical and adhesion properties of a clear polyester powder coating. Prog Org Coat 76:1625–1632
4. Mirhosseini SS, Razavi RS, Taheran M, Barekat M (2016) Wear behavior of polyurethane/carbon black coatings on 6061 aluminum alloy substrates. Prog Org Coat 97:37–43
5. Yuan R, Wu S, Wang B, Liu Z, Mu L, Ji T, Chen L, Liu B, Wang H, Zhu J (2016) Superamphiphobicity and electroactivity enabled dual physical/chemical protections in novel anticorrosive nanocomposite coatings. Polymer 85:37–46
6. Lu Y, Sathasivam S, Song J, Crick CR, Carmalt CJ, Parkin IP (2015) Robust self-cleaning surfaces that function when exposed to either air or oil. Science 347:1132–1135
7. Li H, Yu S, Han X (2016) Fabrication of CuO hierarchical flower-like structures with biomimetic superamphiphobic, self-cleaning and corrosion resistance properties. Chem Eng J 283:1443–1454
8. Wu X, Wyman I, Zhang G, Lin J, Liu Z, Wang Y, Hu H (2016) Preparation of superamphiphobic polymer-based coatings via spray-and dip-coating strategies. Prog Org Coat 90:463–471
9. Wang H, Yan L, Gao D, Liu D, Wang C, Sun L, Zhu Y (2014) Tribological properties of superamphiphobic PPS/PTFE composite coating in the oilfield produced water. Wear 319:62–68
10. Jiang W, Grozea CM, Shi Z, Liu G (2014) Fluorinated raspberry-like polymer particles for superamphiphobic coatings. ACS Appl Mater Interfaces 6:2629–2638
11. Ge B, Zhang Z, Men X, Zhu X, Zhou X (2014) Sprayed superamphiphobic coatings on copper substrate with enhanced corrosive resistance. Appl Surf Sci 293:271–274
12. Deng X, Mammen L, Butt HJ, Vollmer D (2012) Candle soot as a template for a transparent robust superamphiphobic coating. Science 335:67–70
13. Chu Z, Seeger S (2014) Superamphiphobic surfaces. Chem Soc Rev 43:2784–2798
14. Tuominen M, Teisala H, Haapanen J, Mäkelä JM, Honkanen M, Vippola M, Bardage S, Wålinderg MEP, Swerin A (2016) Superamphiphobic overhang structured coating on a biobased material. Appl Surf Sci 389:135–143
15. Saifaldeen ZS, Khedir KR, Camci MT, Ucar A, Suzer S, Karabacak T (2016) The effect of polar end of long-chain fluorocarbon oligomers in promoting the superamphiphobic property over multi-scale rough al alloy surfaces. Appl Surf Sci 379:55–65
16. Peng P, Shi B, Lan Y (2011) Preparation of PDMS-silica nanocomposite membranes with silane coupling for recovering ethanol by pervaporation. Sep Sci Technol 46:420–427
17. Yuan Z, Bin J, Wang X, Wang M, Huang J, Peng C, Xing S, Xiao J, Zeng J, Xiao X, Fu X (2014) Preparation of a polydimethylsiloxane (PDMS)/$CaCO_3$ based superhydrophobic coating. Surf Coat Technol 254:97–103
18. Kapridaki C, Maravelaki-Kalaitzaki P (2013) TiO_2-SiO_2-PDMS nano-composite hydrophobic coating with self-cleaning properties for marble protection. Prog Org Coat 76:400–410
19. Chakradhar RPS, Kumar VD, Rao JL, Basu BJ (2011) Fabrication of superhydrophobic surfaces based on ZnO-PDMS nanocomposite coatings and study of its wetting behaviour. Appl Surf Sci 257: 8569–8575
20. Gao N, Yan YY, Chen XY, Mee DJ (2011) Superhydrophobic surfaces with hierarchical structure. Mater Lett 65:2902–2905
21. Nine MJ, Cole MA, Johnson L, Tran DNH, Losic D (2015) Robust superhydrophobic graphene-based composite coatings with self-cleaning and corrosion barrier properties. ACS Appl Mater Interfaces 7:28482–28493
22. Park S, An J, Potts JR, Velamakanni A, Murali S, Ruoff RS (2011) Hydrazine-reduction of graphite- and graphene oxide. Carbon 49: 3019–3023
23. Zamanizadeh HR, Shishesaz MR, Danaee I, Zaarei D (2015) Investigation of the corrosion protection behavior of natural montmorillonite clay/bitumen nanocomposite coatings. Prog Org Coat 78:256–260
24. Lai M-C, Chang K-C, Yeh J-M, Liou S-J, Hsieh M-F, Chang H-S (2007) Advanced environmentally friendly anticorrosive materials prepared from water-based polyacrylate/Na^+-MMT clay nanocomposite latexes. Eur Polym J 43:4219–4228
25. Zhang Y, Shao Y, Zhang T, Meng G, Wang F (2013) High corrosion protection of a polyaniline/organophilic montmorillonite coating for magnesium alloys. Prog Org Coat 76:804–811
26. Meera KMS, Sankar RM, Murali A, Jaisankar SN, Mandal AB (2012) Sol-gel network silica/modified montmorillonite clay hybrid nanocomposites for hydrophobic surface coatings. Colloid Surf B 90:204–210
27. Tuukka T, Bower C, Andrew P, Franssila S, Ikkala O, Ras RHA (2011) Mechanically durable superhydrophobic surfaces. Adv Mater 23:673–678
28. Xiu Y, Liu Y, Hess DW, Wong CP (2010) Mechanically robust superhydrophobicity on hierarchically structured Si surfaces. Nanotechnology 21:155705

29. Barbero DR, Saifullah MSM, Hoffmann P, Mathieu HJ, Anderson D, Jones GAC, Welland ME, Steiner U (2007) High-resolution nanoimprinting with a robust and reusable polymer mold. Adv Funct Mater 17:2419–2425
30. Yuan R, Wu S, Yu P, Wang B, Mu L, Zhang X, Zhu Y, Wang B, Wang H, Zhu J (2016) Superamphiphobic and electroactive nanocomposite towards self-cleaning, anti-wear and anti-corrosion coatings. ACS Appl Mater Interfaces 8:12481–12493
31. Zhou M, Liu Q, Wu S, Gou Z, Wu X, Xu D (2016) Starch/chitosan films reinforced with polydopamine modified MMT: effects of dopamine concentration. Food Hydrocoll 61:678–684
32. Yang C, Zhang Q, Li J, Gao R, Li Z, Huang W (2016) Catalytic activity and crystal structure modification of Pd/γ-Al_2O_3-TiO_2 catalysts with different Al_2O_3 contents. J Energy Chem 25:375–380
33. Kumar AM, Gasem ZM (2015) In situ electrochemical synthesis of polyaniline/*f*-MWCNT nanocomposite coatings on mild steel for corrosion protection in 3.5% NaCl solution. Prog Org Coat 78: 387–394
34. Peng C-W, Chang K-C, Weng C-J, Lai M-C, Hsu C-H, Hsu S-C, Hsu Y-Y, Hung W-I, Wei Y, Yeh J-M (2013) Nano-casting technique to prepare polyaniline surface with biomimetic superhydrophobic structures for anticorrosion application. Electrochim Acta 95:192–199
35. Hinderliter BR, Croll SG, Tallman DE, Su Q, Bierwagen GP (2006) Interpretation of EIS data from accelerated exposure of coated metals based on modeling of coating physical properties. Electrochim Acta 51:4505–4515
36. Zhang D, Qian H, Wang L, Li X (2016) Comparison of barrier properties for a superhydrophobic epoxy coating under different simulated corrosion environments. Corros Sci 103:230–241